Hindawi Publishing Corporation
Journal of Nanomaterials
Volume 2014, Article ID 180765, 8 pages
http://dx.doi.org/10.1155/2014/180765

Research Article

Enhanced Light Output of Dipole Source in GaN-Based Nanorod Light-Emitting Diodes by Silver Localized Surface Plasmon

Huamao Huang,[1] Haiying Hu,[2] Hong Wang,[1] and Kuiwei Geng[3]

[1] *Engineering Research Center for Optoelectronics of Guangdong Province, School of Physics and Optoelectronics, South China University of Technology, Guangzhou, Guangdong 510640, China*
[2] *School of Civil and Transportation Engineering, South China University of Technology, Guangzhou, Guangdong 510640, China*
[3] *School of Electronics and Information Engineering, South China University of Technology, Guangzhou, Guangdong 510640, China*

Correspondence should be addressed to Hong Wang; phhwang@scut.edu.cn

Received 20 July 2014; Accepted 6 August 2014; Published 20 August 2014

Academic Editor: Xijin Xu

The light output of dipole source in three types of light-emitting diodes (LEDs), including the conventional planar LED, the nanorod LED, and the localized surface plasmon (LSP) assisted LED by inserting silver nanoparticles in the gaps between nanorods, was studied by use of two-dimensional finite difference time domain method. The height of nanorod and the size of silver nanoparticles were variables for discussion. Simulation results show that a large height of nanorod induces strong wavelength selectivity, which can be significantly enhanced by LSP. On condition that the height of nanorod is 400 nm, the diameter of silver nanoparticle is 100 nm, and the wavelength is 402.7 nm, the light-output efficiency for LSP assisted LED is enhanced by 190% or 541% as compared to the nanorod counterpart or the planar counterpart, respectively. The space distribution of Poynting vector was present to demonstrate the significant enhancement of light output at the resonant wavelength of LSP.

1. Introduction

High-efficiency GaN-based light-emitting diode (LED) has tremendous potential for general lighting. However, in conventional planar epilayers, the InGaN/GaN multiple quantum well (MQW) contains large strain, which would induce a high dislocation density and piezoelectric field, due to the mismatches in lattice constant and thermal expansion between heteroepitaxial layers. To mitigate the strain in MQWs, nanorod LEDs were proposed [1]. The active layer is composed of nanoscale rod array in nanorod LEDs instead of planar thin-film in conventional counterparts. A straightforward fabrication method for nanorod LEDs is to etch the planar epilayers with nanoscale patterned mask [2–10]. In these published literatures, most researchers focused on the strain relaxation processes, and few studies were involved in light-output enhancement. To improve the light output, the nanorod LED was annealed in a mixture of N_2 and NH_3 gases [2]. Moreover, the size of the nanorods [6] and the spatial occupation factor of the nanorod sidewall [7], which was defined by the sidewall length over the unetched area of planar epilayer, should be carefully selected. As for the light extraction efficiency, after the alumina powders were spin-coated on the p-GaN layer as mask for etching of nanorod array, the residual alumina particles on the top of nanorods benefit the light extraction efficiency [10].

Localized surface plasmon (LSP) has attracted much attention for the enhancement of light output in LEDs [11–20]. The LSP provides a fast energy transfer channel by coupling the excited dipole energy of MQWs into surface plasmon modes of noble metal particles and consequently enhances the spontaneous emission rate of MQWs, thereby improving the light output of LEDs. However, due to the exponential decay of the LSP evanescent field, the penetration depth of the LSP field into the GaN material is limited to be several tens of nanometers [21]. On the other hand, the p-GaN is generally thicker than 100 nm to maintain p-n junction. In order to place the metal particles within

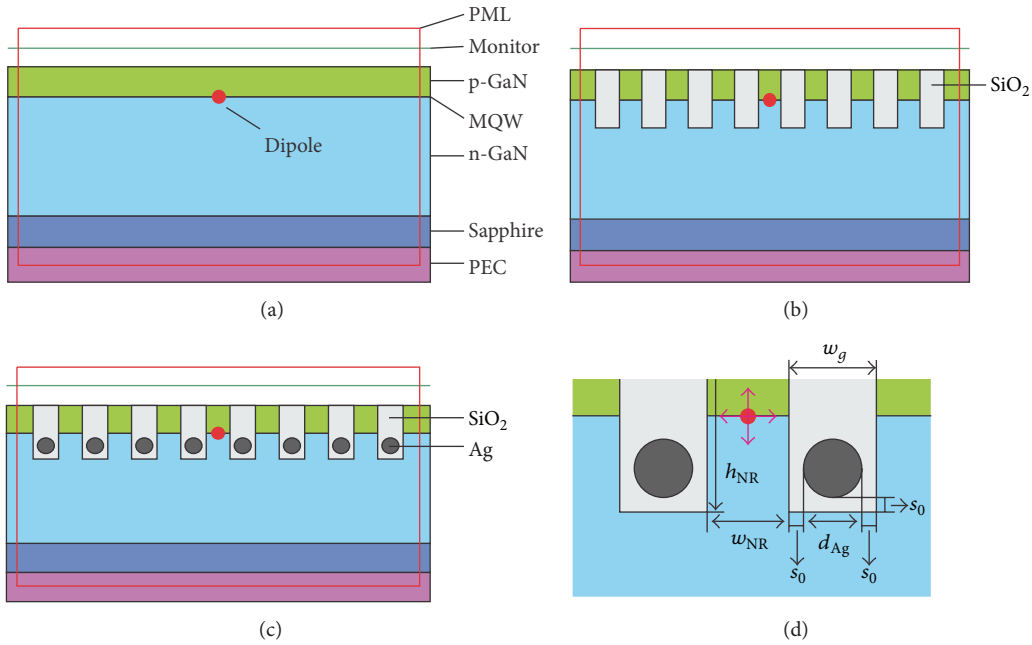

FIGURE 1: Schematic structure of (a) planar LED, (b) nanorod LED, and (c) LSP assisted LED. (d) is an enlarged view of the vicinity of dipole source in (c). The red circle is the dipole source.

the fringing field of MQWs for effective MQW-LSP coupling, the metal particles were embedded into the n-GaN [11–13] or p-GaN [14–17] layers. However, the epitaxial growth process must be interrupted for the fabrication of metal particles and the epilayers following the metal particles may exhibit poor crystal quality. Alternately, after the epitaxial wafer was completely finished, the p-GaN layer was partially etched; if the etching part is thinner enough, the LSP assisted light emission was significantly enhanced [18–20]. For the case of nanorod LEDs, the noble metal particles can be placed in the gaps between the nanorods without additional etching process.

In this paper, the nanorod LEDs with the assistance of silver LSP are proposed, and the light output of dipole source in the planar LED, the nanorod LED, and the LSP assisted LED is studied by two-dimensional finite difference time domain (2D FDTD) method.

2. Materials and Methods

In order to clarify the effects of the nanorod array and the LSP, three types of LED chips shown in Figure 1 were simulated by 2D FDTD method. The first type is the conventional planar LED. The second type is the nanorod LED, in which the nanorod array was achieved by etching part of planar epilayers and filling SiO_2 in the gaps for passivation. The third one is the LSP assisted LED by inserting silver (Ag) nanoparticles in the gaps between nanorods. The width of the nanorods was set to be $w_{NR} = 100$ nm and the height, h_{NR}, was chosen as a variable. The spacing between the Ag nanoparticle and the surrounding SiO_2 sidewall was set to be $s_0 = 10$ nm, as shown in Figure 1(d). This can be realized by employing core-shell Ag/SiO_2 nanoparticles. The widths of gaps were set to be $w_g = d_{Ag} + 2 \times s_0$, where d_{Ag} is the diameter of Ag nanoparticles. In order to reduce the computation resource [22], our model is only composed of four layers, including a 0.2 μm thick p-GaN layer, a 2 μm thick n-GaN layer, a 1 μm thick sapphire substrate, and a perfect electrical conductor (PEC) layer. The MQW layer was simplified as the interface between the two types of GaN layers, and the electric point dipole was chosen as the source for spontaneous emission. The dipole source was placed at the middle of the horizontal axis of the chip, of which the width was set to be $w_{chip} = 5.22$ μm and the nanorods were in symmetric distribution with regard to the dipole source. Due to the isotropic emission feature, two orthogonal orientations of dipole source shown in Figure 1(d) were considered [22]. The mesh grids in the vicinity of the dipole source and the Ag nanoparticles were set to be 1 nm. The power monitor was placed at 0.45 μm distance from the top surface of p-GaN layer. The perfect matched layer (PML) boundaries were used and the maximum simulation time was set to be a large value of 2 000 fs, while the simulation would automatically shut off early when the total energy within the simulation domain drops to 1×10^{-8} of the maximum energy injected.

The material parameters used in our simulation were from experimental data [23, 24]. However, the discrete experimental data should be represented by a continuous function in FDTD simulation. Using the multicoefficient fitting algorithm [25], the refractive indices of Ag [23] and GaN [24] in the wavelength range from 300 nm to 800 nm can be described by an analytic model, and the fitting curves are

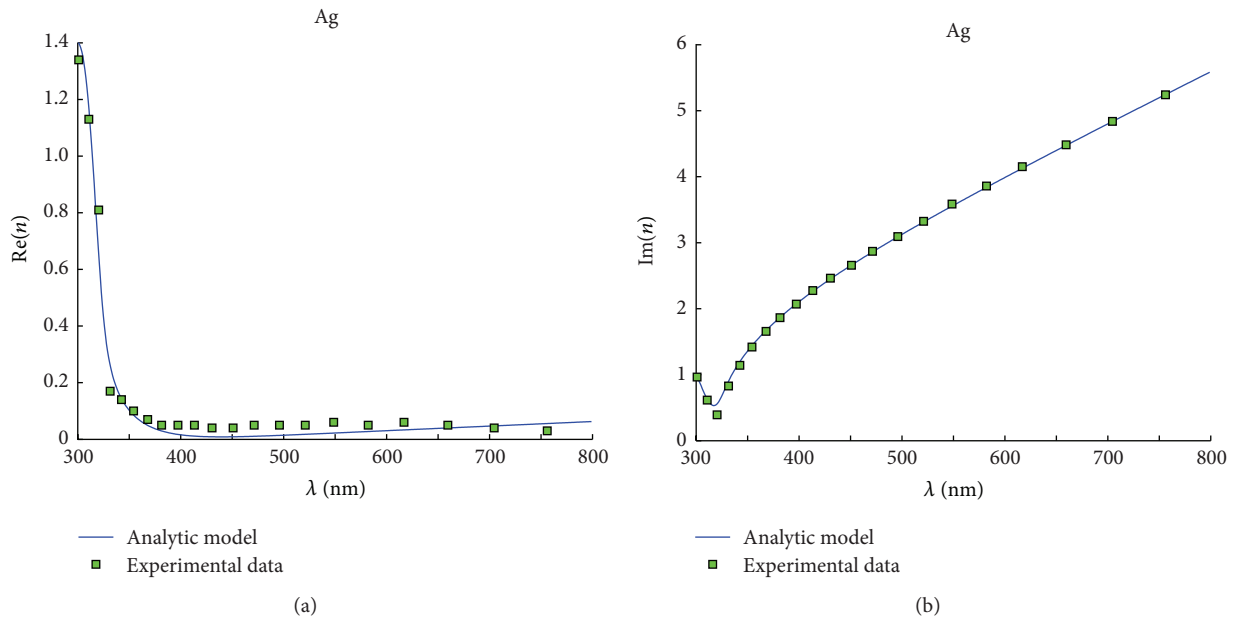

Figure 2: The experimental data and fitting curves of (a) the real part and (b) the imaginary part of refractive index, n, of Ag.

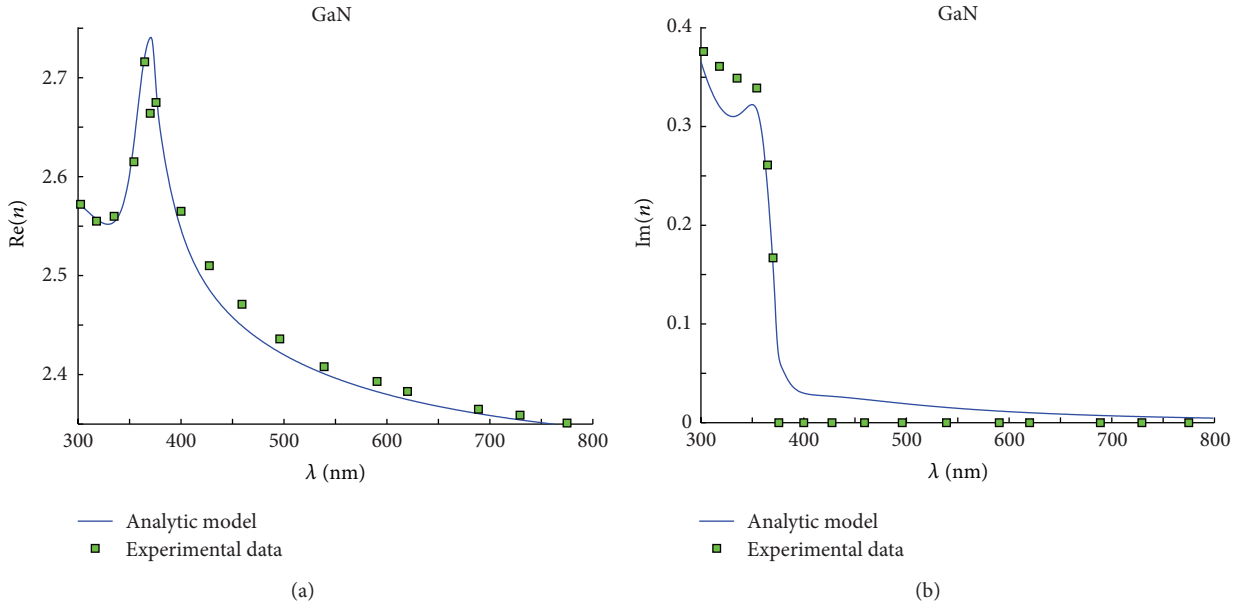

Figure 3: The experimental data and fitting curves of (a) the real part and (b) the imaginary part of refractive index, n, of GaN.

shown in Figures 2 and 3. On the other hand, the refractive indices of sapphire and SiO_2 were constants of 1.78084 and 1.46665, respectively.

Since the dipole-LSP coupling is strongly depending on the distance and the particle size, the h_{NR} varied from 100 nm to 500 nm with the interval of 100 nm, and the d_{Ag} varied from 20 nm to 200 nm with the interval of 20 nm. Because the w_{chip} was fixed while d_{Ag} varied, the number of nanorods, $m_{NR} = 2 \times \text{floor}\{(1/2)w_{chip}/(w_{NR} + d_{Ag} + 2s_0)\}$, in each serial of simulation was also a variable, where floor$\{x\}$ was the arithmetic operation to find the closest integer less than x. The minimal value of m_{NR} was calculated as 16 for d_{Ag} = 200 nm, while the maximum was 36 for d_{Ag} = 20 nm.

3. Results and Discussion

Figure 4 shows the light-output efficiency, η, which was defined by light-output power normalized to the source power. It is shown from the left column of figures, Figure 4(a), that the η for planar LEDs are always less than 17%. A high degree of coincidence of $\eta(\lambda)$ curves for various h_{NR} and d_{Ag}

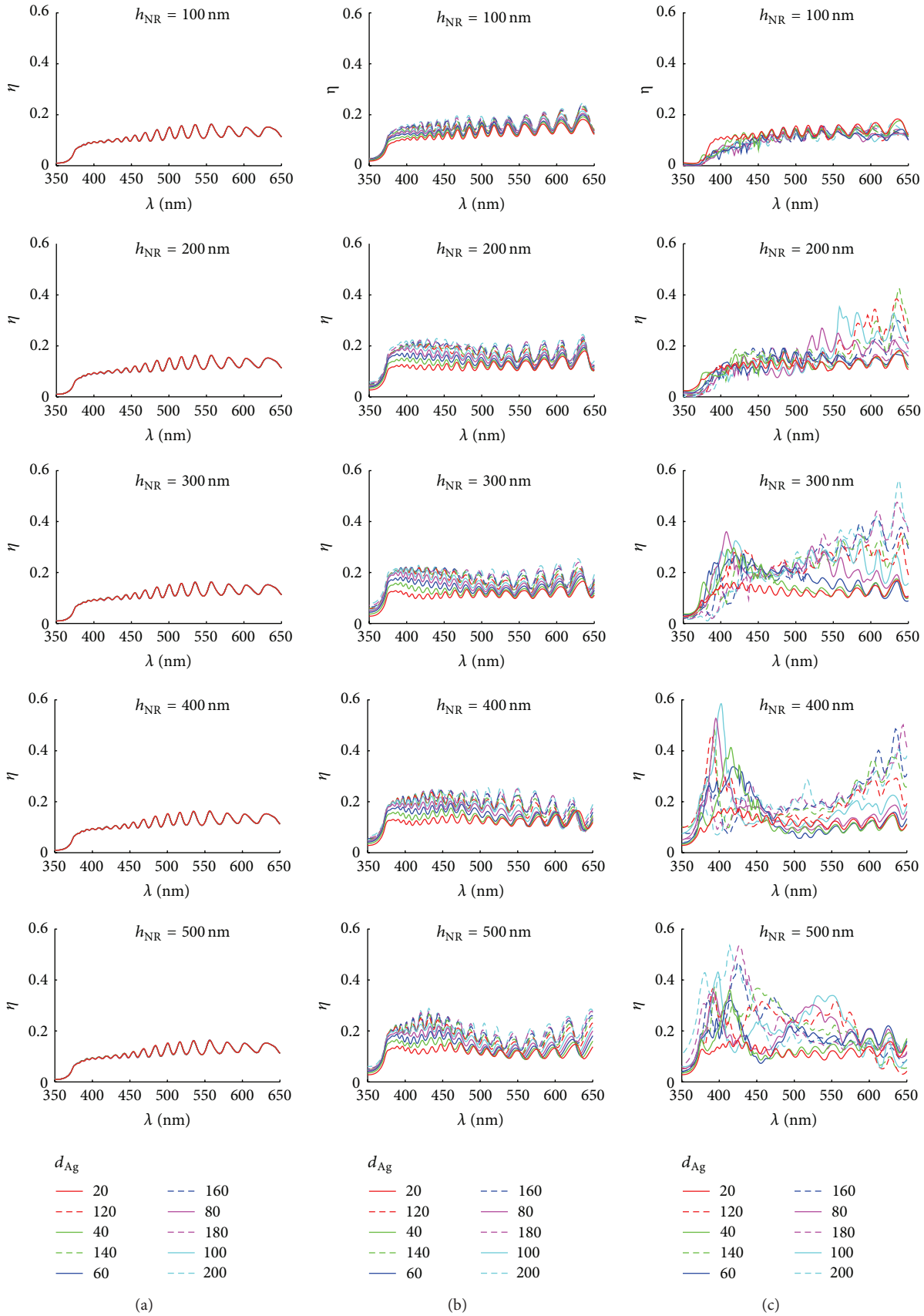

FIGURE 4: The light-output efficiency of dipole source, η, in (a) planar LED, (b) nanorod LED, and (c) LSP assisted LED, where h_{NR} = [100, 200, 300, 400, 500] nm and d_{Ag} = [20, 40, 60, . . . , 200] nm.

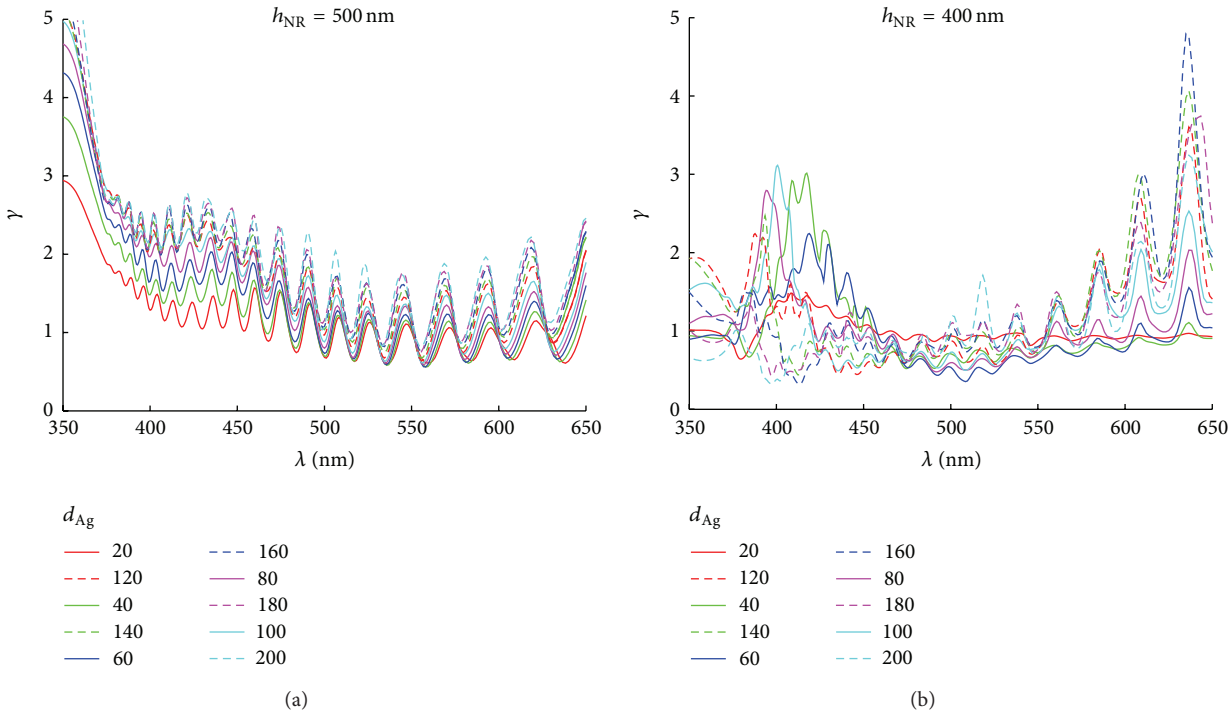

FIGURE 5: The enhancement of the light-output efficiency, γ, for (a) nanorod LEDs as compared to planar LEDs at h_{NR} = 500 nm and (b) LSP assisted LEDs as compared to nanorod LEDs at h_{NR} = 400 nm, where d_{Ag} = [20, 40, 60, ..., 200] nm. Note that $\gamma > 1$ means the enhancement while $\gamma < 1$ is the degradation.

shows that the calculation errors coming from the different mesh grids can be ignored.

Figure 4(b) shown in the middle column are the results for nanorod LEDs. Generally, the η increases as the d_{Ag} increases because of the larger surface area and reduced absorption of GaN material. On the condition of h_{NR} = 100 nm, all η over the whole wavelength range for nanorod LEDs are higher than that for planar counterparts, which imply that the short nanorod does not induce strong resonance oscillation at specific wavelength and mainly provides scattering centers. However, if h_{NR} increases, the strong wavelength selectivity occurs. The η fluctuates intensively and the fluctuation is expanded with the increasing of h_{NR}, d_{Ag}, and λ. The η in the short wavelength range, e.x. from 400 nm to 470 nm, exhibits significant enhancement, especially in the case of d_{Ag} being 500 nm. The maximal value of η for nanorod LED is 28.9%, which is enhanced by 108% compared to the planar counterpart, in the case of h_{NR} = 500 nm, d_{Ag} = 200 nm, and λ = 431.65 nm, as shown in Figure 5(a). However, in specific domain of longer wavelength range, the η is reduced as compared to the planar LED. For example, as shown in Figure 5(a), in the case of h_{NR} = 500 nm and d_{Ag} = 20 nm, the η for nanorod LED is less than that for planar LED in the wavelength range from 550.5 nm to 568.5 nm.

The results for LSP assisted LED are shown in Figure 4(c) in the right column. On the condition of h_{NR} = 100 nm, the η for LSP assisted LED are always lower than nanorod counterparts, except the case of d_{Ag} = 20 nm. This can be ascribed to the competition of the absorption loss from Ag material and the scattering effect from Ag metal mirror. The absorption loss is always the dominant effect unless the particle size is small enough. If h_{NR} increases, the LSP takes effect and provides significant wavelength selectivity. With the increasing of h_{NR} from 200 nm to 500 nm, the significant enhancement of η appears firstly in the long wavelength, e.x. nearby 610 nm, then in short wavelength, e.x. nearby 400 nm, and later in middle wavelength range, e.x. nearby 535 nm. The maximal value of η for LSP assisted LED is 58.5%, which is enhanced by 190% compared to the nanorod counterpart, in the case of h_{NR} = 400 nm, d_{Ag} = 100 nm, and λ = 402.7 nm, as shown in Figure 5(b). As compared to the planar counterpart, this η is enhanced by 541%. Note that the maximum of η shown in Figure 4(c) and the maximal value of γ, which is the enhancement of η, shown in Figure 5(b) do not coincide. On the other hand, the suppressing of η still exists. For example, as shown in Figure 5(b), in the case of h_{NR} = 400 nm and d_{Ag} less than 120 nm, the η for LSP assisted LED is less than that for planar LED in the wavelength range from 460 nm to 555 nm.

The η was estimated by the average value of independent simulation results for each orientation of the dipole source shown in Figure 1(d). To further understand the effects of LSP on different polarization of dipole source, the magnitude of Poynting vector at the wavelength of 402.7 nm and 460 nm is shown in Figures 6 and 7 in the case of h_{NR} = 400 nm and d_{Ag} = 100 nm. As shown in Figure 4, for LSP assisted LED, the η reached maximum at λ = 402.7 nm, while the η at λ = 460 nm is a relative small value.

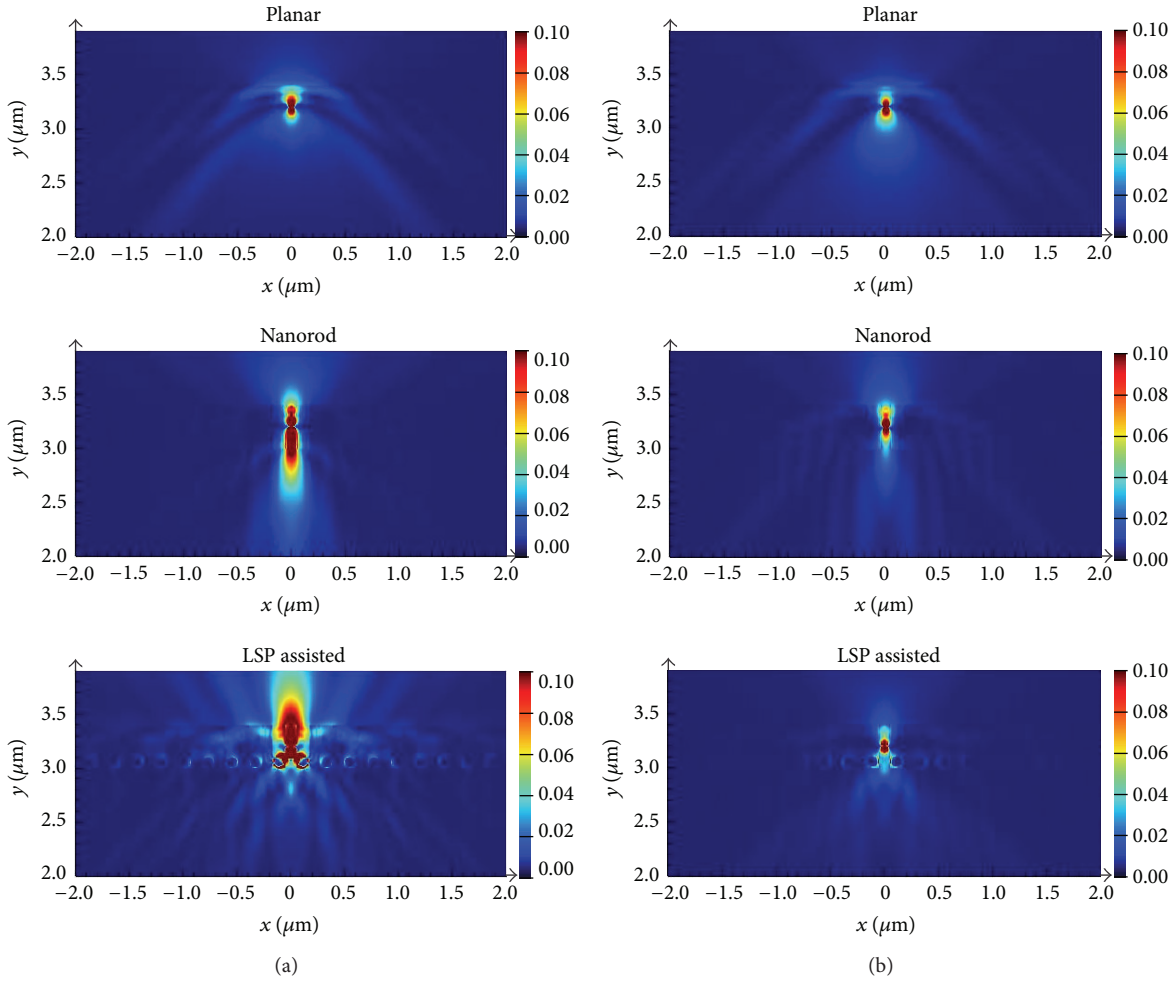

FIGURE 6: As the polarization of dipole source is along the horizontal direction, the magnitude of Poynting vector at the wavelength of (a) 402.7 nm and (b) 460 nm, where h_{NR} = 400 nm and d_{Ag} = 100 nm.

Figure 6 shows the magnitude of Poynting vector as the polarization of dipole source is along the horizontal direction. It is shown that the light energy is confined well in the planar LEDs at the two wavelengths. Two diffraction orders can be observed due to the planar structure. For the nanorod LEDs, most of the light energy is restricted in the nanorod. Due to the strong resonance oscillation at the wavelength of 402.7 nm, the light energy is much higher than that at the wavelength of 460 nm. In addition, lots of light energy leaks out of the nanorod downward to the n-GaN layer, but the light energy which escaped from the top surface is still limited. In the case of LSP assisted LEDs, the significant enhancement of light output is achieved at the resonant wavelength of 402.7 nm. Since the dipole source is placed above the Ag nanoparticles, the LSP is mainly located on the top surface of nanoparticles, and thus the lights generated from the LSP escape from the chip via the top surface; thereby the downward-leaking light energy is suppressed. For the detuning wavelength of 460 nm, the Ag nanoparticles do not produce the LSP but provide the reflective effects and surfer absorption loss; therefore, the light output at 460 nm for LSP assisted LED is less than that for nanorod LED.

As shown in Figure 7, on condition that the polarization of dipole source is along the perpendicular direction, the results are similar to the horizontal-polarization case shown in Figure 6. The light energy from the dipole source with perpendicular polarization expands widely toward left side and right side, and thus the confinement effects from the nanorod and the dipole-LSP coupling from the Ag nanoparticles are reduced. Consequently, the light output from the dipole source with perpendicular polarization is less than that with horizontal polarization.

4. Conclusion

In summary, the light output of dipole source which escaped from planar LED, nanorod LED, and LSP assisted LED is studied by use of 2D FDTD method. The maximal value of light-output efficiency for LSP assisted LED is enhanced by 190% or 541% as compared to the nanorod counterpart or the planar counterpart, respectively. The significant enhancement of light output at the resonant wavelength of LSP was demonstrated by the space distribution of

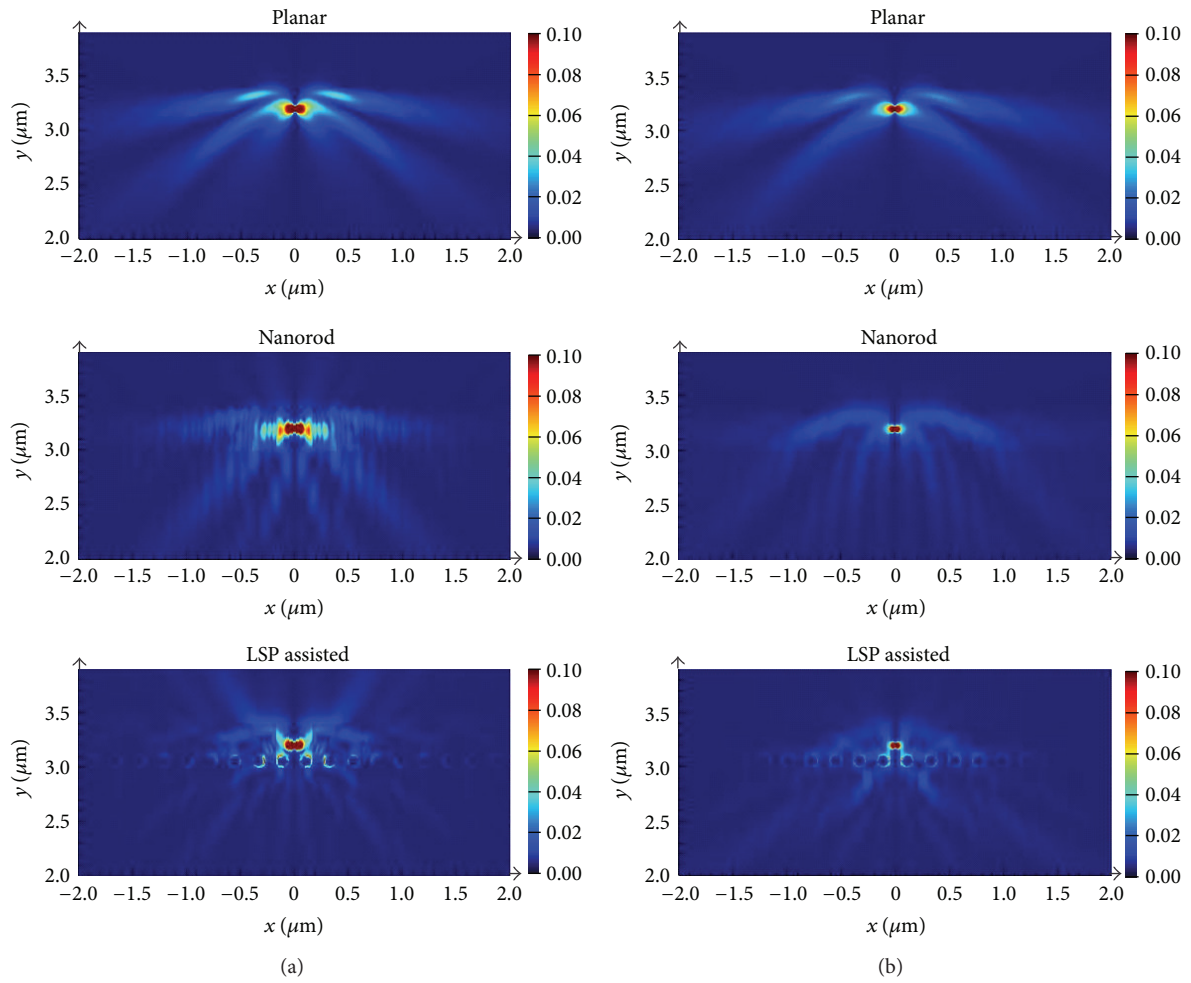

FIGURE 7: As the polarization of dipole source is along the perpendicular direction, the magnitude of Poynting vector at the wavelength of (a) 402.7 nm and (b) 460 nm, where $h_{NR} = 400$ nm and $d_{Ag} = 100$ nm.

the Poynting vector. Although only the dipole-LSP coupling was considered in this paper, these results can be extended to the MQW-LSP coupling, since the MQW can be modeled by multiple electric dipole sources located in specific positions with orthogonal polarizations.

Conflict of Interests

The authors declare that there is no conflict of interests regarding the publication of this paper.

Acknowledgments

This work was supported by the National High Technology Research and Development Program of China (863 Program) (no. 2014AA032609), the Strategic Emerging Industry Special Funds of Guangdong Province (no. 2011A081301004, no. 2012A080302003, and no. 2012A080304015), the Key Technologies R&D Program of Guangzhou City (no. 2011Y5-00006), and the Fundamental Research Funds for the Central Universities (no. 2013ZM093 and no. 2013ZP0017).

References

[1] S. Li and A. Waag, "GaN based nanorods for solid state lighting," *Journal of Applied Physics*, vol. 111, no. 7, Article ID 071101, 2012.

[2] S. Keller, C. Schaake, N. A. Fichtenbaum et al., "Optical and structural properties of GaN nanopillar and nanostripe arrays with embedded InGaN/GaN multi-quantum wells," *Journal of Applied Physics*, vol. 100, no. 5, Article ID 054314, 2006.

[3] C. H. Chiu, T. C. Lu, H. W. Huang et al., "Fabrication of InGaN/GaN nanorod light-emitting diodes with self-assembled Ni metal islands," *Nanotechnology*, vol. 18, no. 44, Article ID 445201, 2007.

[4] C.-Y. Wang, L.-Y. Chen, G.-P. Chen et al., "GaN nanorod light emitting diode arrays with a nearly constant electroluminescent peak wavelength," *Optics Express*, vol. 16, no. 14, pp. 10549–10556, 2008.

[5] H. Ono, Y. Ono, K. Kasahara, J. Mizuno, and S. Shoji, "Fabrication of high-intensity light-emitting diodes using nanostructures by ultraviolet nanoimprint lithography and electrodeposition," *Japanese Journal of Applied Physics*, vol. 47, no. 2, pp. 933–935, 2008.

[6] Y.-R. Wu, C. Chiu, C.-Y. Chang, P. Yu, and H.-C. Kuo, "Size-dependent strain relaxation and optical characteristics of

InGaN/GaN nanorod LEDs," *IEEE Journal of Selected Topics in Quantum Electronics*, vol. 15, no. 4, pp. 1226–1233, 2009.

[7] V. Ramesh, A. Kikuchi, K. Kishino, M. Funato, and Y. Kawakami, "Strain relaxation effect by nanotexturing InGaN/GaN multiple quantum well," *Journal of Applied Physics*, vol. 107, no. 11, Article ID 114303, 2010.

[8] Q. Li, K. R. Westlake, M. H. Crawford et al., "Optical performance of top-down fabricated InGaN/GaN nanorod light emitting diode arrays," *Optics Express*, vol. 19, no. 25, pp. 25528–25534, 2011.

[9] Q. Wang, J. Bai, Y. P. Gong, and T. Wang, "Influence of strain relaxation on the optical properties of InGaN/GaN multiple quantum well nanorods," *Journal of Physics D: Applied Physics*, vol. 44, no. 39, Article ID 395102, 2011.

[10] S. H. Kim, H. H. Park, Y. H. Song et al., "An improvement of light extraction efficiency for GaN-based light emitting diodes by selective etched nanorods in periodic microholes," *Optics Express*, vol. 21, no. 6, pp. 7125–7130, 2013.

[11] M.-K. Kwon, J.-Y. Kim, B.-H. Kim et al., "Surface-plasmon-enhanced light-emitting diodes," *Advanced Materials*, vol. 20, no. 7, pp. 1253–1257, 2008.

[12] L.-W. Jang, J.-W. Ju, D.-W. Jeon et al., "Enhanced light output of InGaN/GaN blue light emitting diodes with Ag nano-particles embedded in nano-needle layer," *Optics Express*, vol. 20, no. 6, pp. 6036–6041, 2012.

[13] M. K. Kwon, J. Y. Kim, and S. J. Park, "Enhanced emission efficiency of green InGaN/GaN multiple quantum wells by surface plasmon of Au nanoparticles," *Journal of Crystal Growth*, vol. 370, pp. 124–127, 2013.

[14] C.-Y. Cho, M.-K. Kwon, S.-J. Lee et al., "Surface plasmon-enhanced light-emitting diodes using silver nanoparticles embedded in p-GaN," *Nanotechnology*, vol. 21, no. 20, Article ID 205201, 2010.

[15] C.-Y. Cho, K. S. Kim, S.-J. Lee et al., "Surface plasmon-enhanced light-emitting diodes with silver nanoparticles and SiO_2 nanodisks embedded in *p*-GaN," *Applied Physics Letters*, vol. 99, no. 4, Article ID 041107, 2011.

[16] C. Cho, S. Lee, J. Song et al., "Enhanced optical output power of green light-emitting diodes by surface plasmon of gold nanoparticles," *Applied Physics Letters*, vol. 98, no. 5, Article ID 051106, 2011.

[17] S. Hong, C. Cho, S. Lee et al., "Localized surface plasmon-enhanced nearultraviolet emission from InGaN/GaN lightemitting diodes using silver and platinum nanoparticles," *Optics Express*, vol. 21, no. 3, pp. 3138–3144, 2013.

[18] C. C. Kao, Y. K. Su, C. L. Lin, and J. J. Chen, "Localized surface plasmon-enhanced nitride-based light-emitting diode with Ag nanotriangle array by nanosphere lithography," *IEEE Photonics Technology Letters*, vol. 22, no. 13, pp. 984–986, 2010.

[19] C. Lu, C. Lan, Y. Lai, Y. Li, and C. Liu, "Enhancement of green emission from InGaN/GaN multiple quantum wells via coupling to surface plasmons in a two-dimensional silver array," *Advanced Functional Materials*, vol. 21, no. 24, pp. 4719–4723, 2011.

[20] C.-H. Lu, S.-E. Wu, Y.-L. Lai, Y.-L. Li, and C.-P. Liu, "Improved light emission of GaN-based light-emitting diodes by efficient localized surface plasmon coupling with silver nanoparticles," *Journal of Alloys and Compounds*, vol. 585, pp. 460–464, 2014.

[21] K. Okamoto, I. Niki, A. Shvartser, Y. Narukawa, T. Mukai, and A. Scherer, "Surface-plasmon-enhanced light emitters based on InGaN quantum wells," *Nature Materials*, vol. 3, no. 9, pp. 601–605, 2004.

[22] J.-W. Pan, P.-J. Tsai, K.-D. Chang, and Y.-Y. Chang, "Light extraction efficiency analysis of GaN-based light-emitting diodes with nanopatterned sapphire substrates," *Applied Optics*, vol. 52, no. 7, pp. 1358–1367, 2013.

[23] P. B. Johnson and R. W. Christy, "Optical constants of the noble metals," *Physical Review B*, vol. 6, no. 12, pp. 4370–4379, 1972.

[24] Filmetrics, "Refractive index database," 2014, http://www.filmetrics.com/refractive-index-database.

[25] A. E. Khalifa and M. A. Swillam, "Cheap and efficient plasmonic solar cell," in *Physics, Simulation, and Photonic Engineering of Photovoltaic Devices III, 89811R*, vol. 8981 of *Proceedings of SPIE*, San Francisco, Calif, USA, March 2014.